Kurfess, T.R. and Nagurka, M.L., "A New Visualization of the Evans Root Locus: Gain Plots," Robust Control of Mechanical Systems: Theory and Applications, *ed.* Nwokah, O.D.I., ASME Winter Annual Meeting, Atlanta, GA, December 1-6, 1991, pp. 1-8.

DSC-Vol. 27, Robust Control of Mechanical Systems:
Theory and Applications
ASME 1991

A NEW VISUALIZATION OF THE EVANS ROOT LOCUS: GAIN PLOTS

Thomas R. Kurfess and Mark L. Nagurka
Department of Mechanical Engineering
Carnegie Mellon University
Pittsburgh, Pennsylvania

This paper proposes an alternate graphical representation of the Evans root locus, a well known controls technique for stability and performance evaluation. It shows via a series of transformations a set of Gain Plots (GPs) that depict the polar coordinates, i.e., magnitude and angle, of each closed loop system eigenvalue in the complex plane as a function of proportional gain.

The GPs impart significant insight for determining the values of gain that render a closed–loop system either stable or unstable, and are useful tools for identifying closed–loop designs meeting performance specifications. The GPs are applicable to single–input, single–output and multiple–input, multiple–output feedback systems.

Introduction

In a sequence of landmark papers, W.R. Evans presented a technique for analyzing and graphically portraying the loci of closed–loop system poles (Evans, 1948, 1950). Since the publication of these papers, Evans root locus has become a standard and commonly employed tool of the control engineer. It has several qualities that make it valuable, including the ease with which it may be implemented and the richness of information that it provides.

For most single–input, single–output (SISO) linear time–invariant systems sketching the root locus as a function of gain is a straight-forward task. Most undergraduate controls textbooks present the sketching rules for constructing the root locus plot. By following these rules, the loci of roots or system eigenvalues may be graphed in the complex plane as a system parameter is varied. The most commonly adjusted parameter is the proportional control gain.

This paper promotes an alternate graphical representation of the root locus plot that exposes the relationship between the system eigenvalues and the gain without sacrificing any of the information presented in the standard root locus. The representation is summarized in a pair of Gain Plots (GPs) that casts the magnitude and angle of the system eigenvalues in the complex plane as an explicit function of gain. By displaying eigenvalue polar information, the GPs present system performance in terms of damping ratio and natural frequency in a clear and concise manner. Additionally, eigenvalue sensitivity can be obtained by examining the slopes of the GPs with changing gain. The GPs can be constructed for both SISO and multiple–input, multiple–output (MIMO) systems.

Conceptualization

This section presents a conceptual framework that motivates the development of the GPs. For purposes of illustration, a single "theme" system given by the open–loop transfer function, g(s),

$$g(s) = \frac{(s+3)}{(s+1)(s+2)} \tag{1}$$

is investigated. This plant is embedded in a standard closed–loop negative feedback system shown in Figure 1.

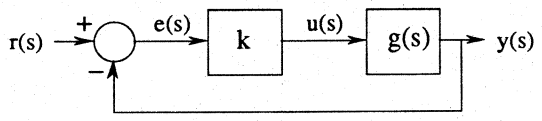

Figure 1. Closed–Loop SISO Negative Feedback Configuration.

The development of the GPs from the root locus plot is paralleled by the development of the Bode plots from the Nyquist diagram. As such, a fundamental relationship appears to exist between the Bode plots, the Nyquist diagram, Evans root locus, and the GPs. A unified framework linking these four controls tools is discussed in the closing section of this paper.

Two Old Friends: 2–Dimensional Nyquist & Root Locus

The Nyquist Diagram (Nyquist, 1932)

The Nyquist diagram is a plot of a sinusoidal transfer function, $g(j\omega)$. The real and imaginary components of $g(j\omega)$ are plotted for $0 \leq \omega < \infty$ where the implicit variable is ω. Figure 2 is the Nyquist diagram of equation (1) for positive ω. The curve starts at $\omega=0$ corresponding to a D.C. gain of 1.5 and phase angle of 0°, and asymptotically approaches the origin (zero magnitude) from –90° as $\omega \rightarrow \infty$.

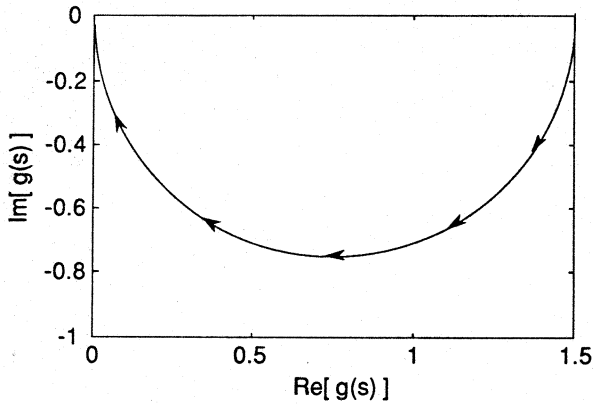

Figure 2. The Nyquist Diagram of Equation (1).

The Evans Root Locus (Evans, 1948, 1950)

The root locus plot shows the location in the complex plane of the characteristic roots, *i.e.*, the eigenvalues, in terms of a (real valued) system parameter such as the proportional gain. It is based on the closed–loop transfer function of Figure 1 given by

$$g_{CL}(s) = \frac{k\, g(s)}{1 + k\, g(s)} \qquad (2)$$

where k is the proportional gain. The stability of the closed–loop system is determined by the eigenvalues, which are the solutions of

$$k\, g(s) = -1 \qquad (3)$$

i.e., the denominator roots of equation (2). The root locus is the solution of equation (3) as the gain k varies in the range $0 \le k < \infty$. Equation (3) is equivalent to two conditions: the angle criterion,

$$\angle k g(s) = \pm 180^{\circ}(2m + 1), \quad m = 0, 1, 2, \ldots \qquad (4)$$

and the magnitude criterion,

$$|k g(s)| = 1 \qquad (5)$$

The root locus plot of equation (1) is shown in Figure 3. Each branch of the root locus starts at k=0 corresponding to a system open–loop pole, and asymptotically approaches either a finite or infinite transmission zero as $k \to \infty$.

By observing if branches enter the right half complex plane, the closed–loop system stability can be determined as the gain varies. In addition, the root locus plot is a graphical performance tool providing metrics of natural frequency and damping ratio. These two characteristics, known from magnitude and angle information, enable the calculation of other performance measures (damped natural frequency, system time constants, *etc.*)

It is possible to show the gain graduation on the locus (with tick marks denoting equal values of k) or to present superimposed constant gain contours. However, even if the root locus is scaled, it is not convenient for determining the gain associated with a given point on the locus. For example, from Figure 3 the gain $k \approx 5.8$ generating the break–in point at $s \approx -4.4$ cannot be determined by inspection.

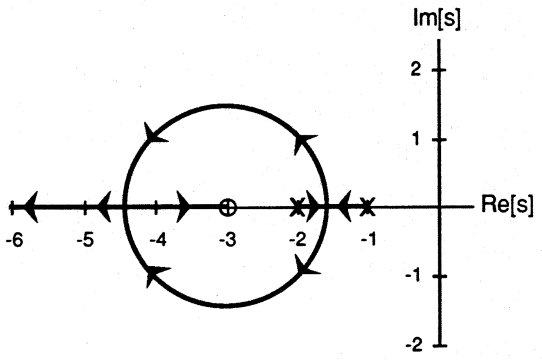

Figure 3. Evans Root Locus Diagram of Equation (1).

Three Dimensional Nyquist and Root Locus

Three Dimensional Nyquist Diagram

The Nyquist diagram can be viewed as the two–dimensional "collapsed" perspective of the three–dimensional curve shown in Figure 4 for the transfer function of equation (1). Here, a third axis is added to the Nyquist plane denoting frequency, ω. Although the three–dimensional curve adds frequency explicitly to the Nyquist diagram, it does not present the controls engineer with an intuitive feel for the system behavior, partly because of the difficulty in following the contour and in extracting coordinate information.

Three Dimensional Root Locus

In a similar manner, the Evans root locus plot can be presented in three–dimensional space where the gain, k, can be displayed on the third axis. Figure 5 presents a three–dimensional root locus for the closed–loop system of Figure 1 with the open–loop transfer function of equation (1). The original Evans root locus is the projection of this three–dimensional locus onto the real–imaginary plane. As before, the three–dimensional representation does not provide the controls engineer with an intuitive feel for system behavior.

Three Dimensional Magnitude and Angle Representations

New three–dimensional representations can be generated by mapping the real and complex components to their magnitude and angle components. Here, the complex value, s,

$$s = \sigma + j\omega = R e^{j\theta} \qquad (6)$$

is expressed in terms of its angle, θ, and magnitude, R,

$$\theta = \tan^{-1}(\omega, \sigma) \quad , \quad R = \sqrt{\sigma^2 + \omega^2} \qquad (7), (8)$$

where θ is given by the two argument inverse tangent function.

Three Dimensional Frequency Plot

Equations (7) and (8) can be used to transform Figure 4 into Figure 6 showing the effect of frequency on the magnitude and angle of the open–loop system given by equation (1). This curve is related to well–known frequency plots (Bode, 1940).

Three Dimensional Gain Plot

Equations (7) and (8) can be used to conformally map Figure 5 into Figure 7 showing the effect of gain on the magnitude and angle

of the closed–loop system assuming the plant of equation (1). This three–dimensional curve is related to the root locus plot.

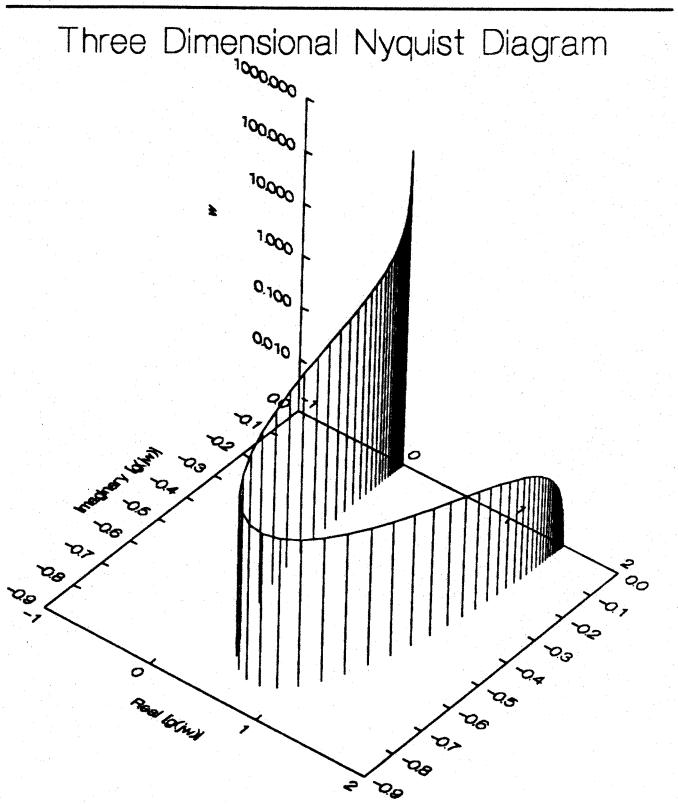

Figure 4. Three Dimensional Nyquist Diagram of Equation (1).

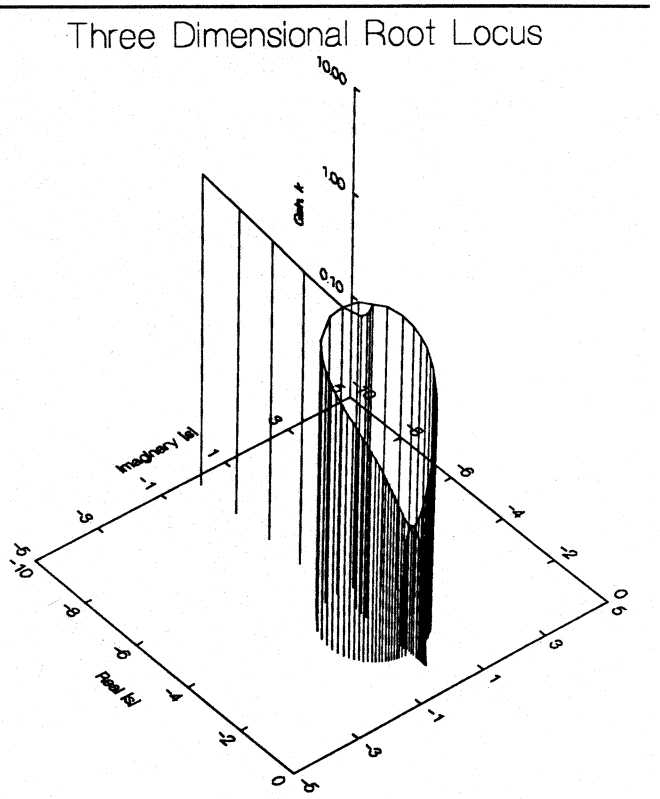

Figure 5. Three Dimensional Evans Root Locus Plot of Equation (1).

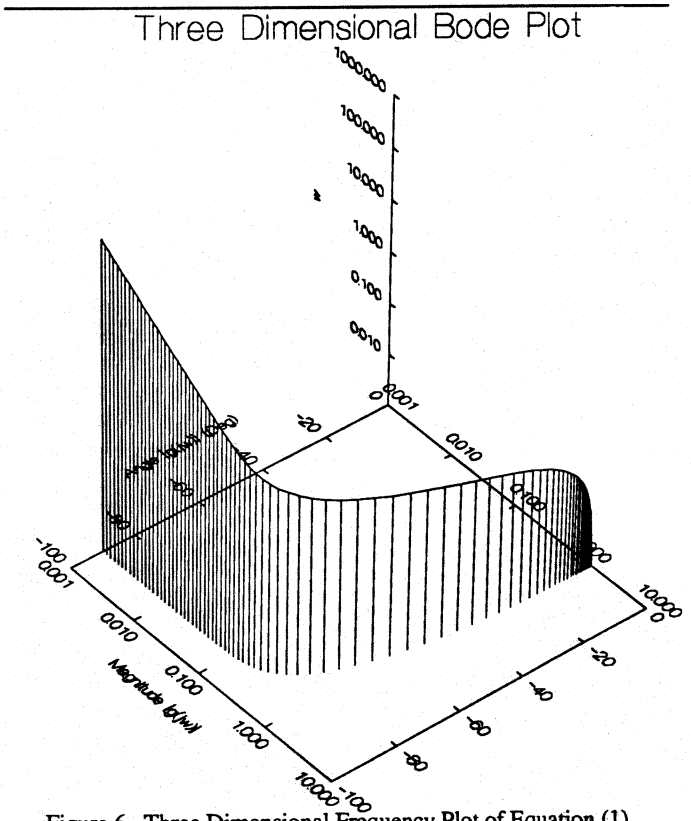

Figure 6. Three Dimensional Frequency Plot of Equation (1).

An Old Friend and a New Friend: Two Dimensional Magnitude and Angle Representations

The Bode Plots (Bode, 1940)

Figures 8a,b are the Bode magnitude and phase (angle) plots, respectively, for the open–loop system given by equation (1). The Bode plots represent two orthogonal views of the three–dimensional frequency plot of Figure 6, *i.e.*, the Bode magnitude plot is seen by observing Figure 6 from a direction orthogonal to the magnitude–ω plane and the Bode phase plot is seen by viewing Figure 6 from a direction orthogonal to the phase–ω plane. Although Figures 6 and 8 were generated using the same data, the projections, *i.e.*, the traditional Bode plots, are significantly simpler to understand.

The Gain Plots (GPs)

Just as Bode plots simplify the three–dimensional frequency plot, GPs elucidate the three–dimensional gain plot. Figures 9a,b are such a representation for the system of equation (1). The Magnitude Gain Plot (MGP) is seen by viewing Figure 7 from a direction orthogonal to the magnitude–k plane and the Angle Gain Plot (AGP) is seen by observing Figure 7 from a direction orthogonal to the angle–k plane. Although the same information is presented in Figures 7 and 9, the GPs are significantly easier to comprehend.

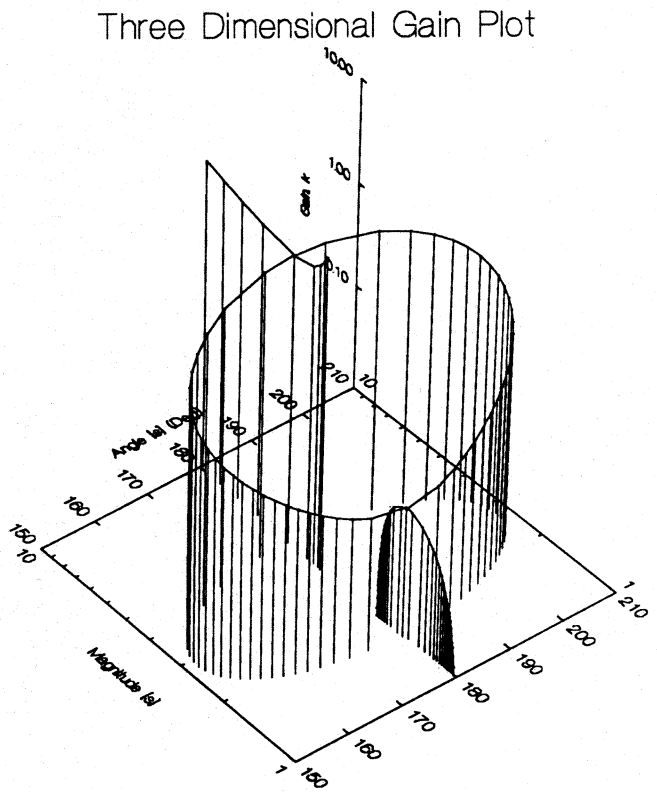

Figure 7. Three Dimensional Gain Plot of Equation (1).

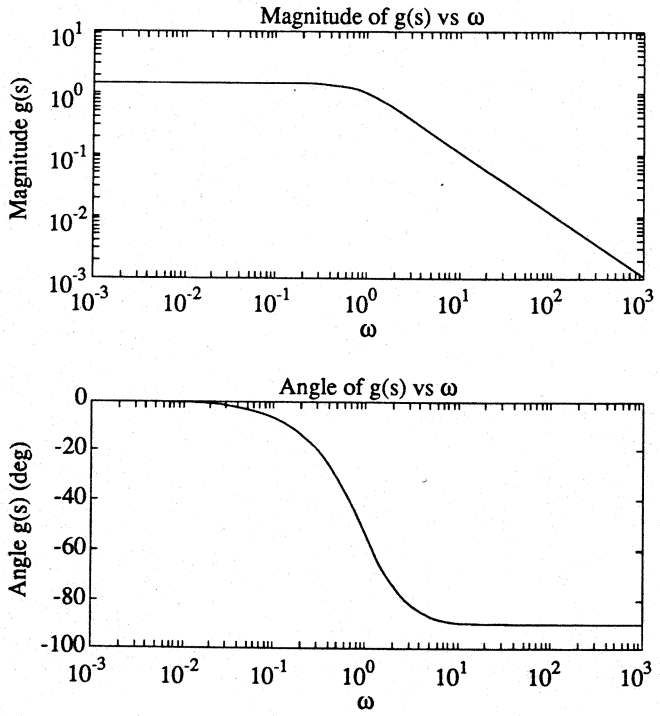

Figure 8. Bode (a) Magnitude and (b) Phase Plot of Equation (1).

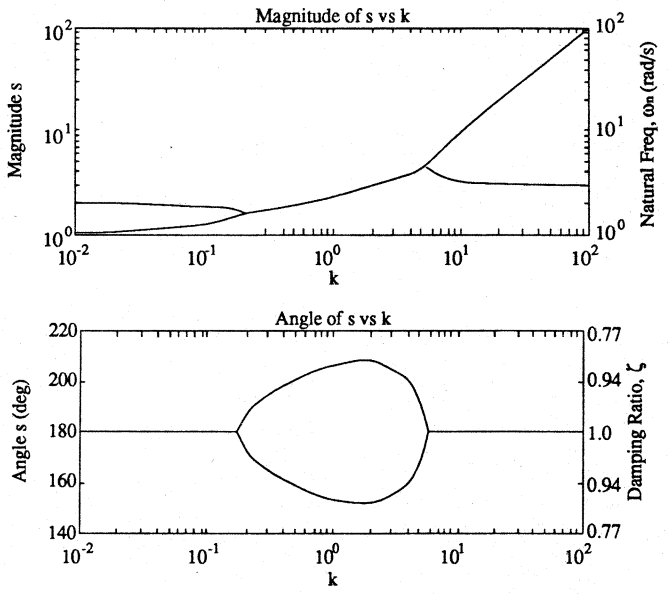

Figure 9. The (a) MGP and (b) AGP of Equation (1).

The AGP reflects the basic construction rule of the root locus, *i.e.*, the angle criterion of equation (4). As a result, the AGP is symmetric along the 180° (= –180°) line. Furthermore, the angle criterion dictates that the eigenvalues must lie on the real axis or be complex conjugates. Thus, a pair of complex conjugate eigenvalues is shown as a single (overlapping) curve in the MGP with corresponding angles symmetrically configured about the 180° line shown in the AGP. As k varies, the complex conjugate eigenvalues may become distinct real eigenvalues, causing their angles to become equal (at a multiple of 180°) and permitting their magnitudes to differ.

The MGP shows two open–loop poles with magnitudes 1 and 2 as $k \rightarrow 0$. It also shows a single finite transmission zero with magnitude 3 and an infinite transmission zero as $k \rightarrow \infty$. The AGP indicates that the two open–loop poles and finite transmission zero are located in the left–half plane since they have angles of 180°. Furthermore, the AGP shows that there is an asymptote of 180° (corresponding to the infinite transmission zero) as $k \rightarrow \infty$.

The GPs highlight the break points corresponding to points where branches leave or enter the real axis of the root locus. For example, these break points occur at $k \approx 0.17$ and at $k \approx 5.83$. Between these break points the AGP indicates that the loci of the two branch points are not on the real axis and the corresponding coincident curves of the MGP confirm that the trajectories are those of a complex conjugate pair.

The GPs present several important stability and performance features of the system; these are summarized in Figure 10. Stability may be determined from the AGP by noting if the angle of an eigenvalue meets the following criterion

$$180°(2m+1) - 90° < |\theta| < 180°(2m+1) + 90° \qquad (9)$$

for m=0, 1, 2, ..., corresponding to a location in the second and third quadrants of the complex plane. For the case m=0, equation (9) simplifies to $90° < \theta < 270°$. This range is shown in the shaded region in Figure 10b.

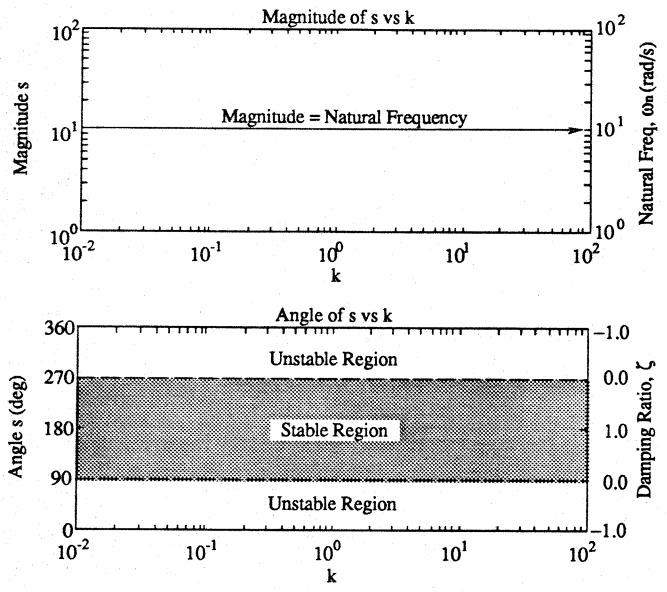

Figure 10. Parameters in the (a) MGP and (b) AGP.

Performance measures are available directly from the GPs. In particular, for complex conjugate eigenvalues the natural frequency, ω_n (rad/s), is the magnitude presented in the MGP, and the damping ratio, $\zeta = -\cos(\theta)$ where θ is the angle in the AGP. In Figure 10, additional axes have been added to display ω_n and ζ in the MGP and AGP, respectively. If the eigenvalues are on the real axis, the MGP presents the system time constants. (Note that negative values of ζ result in unstable systems.)

Although the conventional root locus plot provides such performance information, there are several advantages of the GPs. First, the value of k as an independent variable is represented directly on the abscissa. Hence, the influence of gain on ordinate (dependent) variables is exposed explicitly. Second, the performance measures of ω_n and ζ are provided directly. Thus, given a design specification for ω_n and ζ, the corresponding value(s) of k may be determined by inspection. A novel feature of the GPs is this link of performance and gain.

In addition to these and other advantages (*e.g.*, gain margin, root sensitivity, high gain asymptotic behavior, *etc.*), the GPs provide a unified approach for SISO and MIMO systems where compensation dynamics are governed by a single scalar gain amplifying all plant inputs. MIMO GPs are introduced later in two examples.

Illustrative Examples

This section presents three examples that demonstrate the utility of the GPs.

Non–Trivial SISO Example

Figure 11 is the root locus plot for the negative feedback system of Figure 1 with the open–loop transfer function

$$g(s) = \frac{(s+1)}{s(s-1)(s^2+4s+16)} \qquad (10)$$

(Equation (10) is studied in example A–5–3, Ogata, 1990.) The root locus begins at the open–loop poles located at s={0, +1, $-2 \pm 2\sqrt{3}j$}. The open–loop complex conjugate pole pair migrates to the real axis with increasing gain. One of these poles then proceeds to the finite transmission zero at s=–1; the other pole moves to an infinite transmission zero along an asymptote of 180°. The two real open–loop poles migrate to s≈0.46, and then break out from the real axis. As a complex conjugate pole pair, they move to the left of the imaginary axis. Subsequently, they migrate back to the right of the imaginary axis and continue toward infinite transmission zeros along asymptotes of ±60°. For a small range of k, the root locus is located completely within the left half of the complex plane, corresponding to a stable closed–loop system. This range may be found from the magnitude criterion to be $23.3 < k < 35.7$.

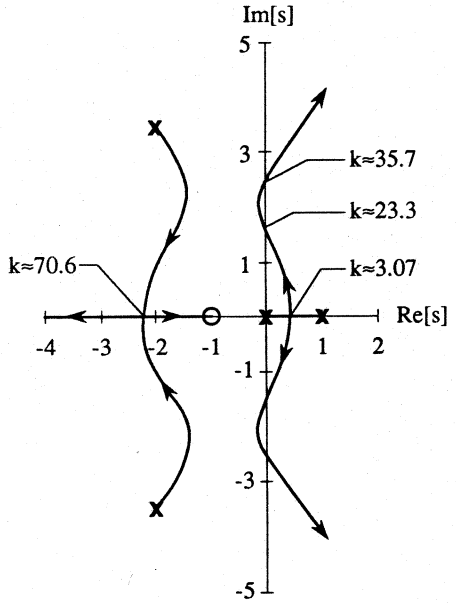

Figure 11. Root Locus for System Given by Equation (10).

Figure 12 shows the GPs for the system given by equation (10). Information about the open–loop eigenvalues at k = 0 shows *(i)* there is an unstable set of open–loop poles at an angle of 0° having magnitudes of 0 and 1, and *(ii)* there is a complex conjugate open–loop pole pair having magnitude 4 at angles of 120° and 240°. By inspection, these complex conjugate poles have a natural frequency of 4 rad/s and a damping ratio of 0.5, although this information is "secondary" since the open–loop system is unstable.

For positive values of gain, the system operates under closed–loop negative feedback and reveals interesting eigenvalue trajectories. For example, the solid and solid dashed lines in the MGP and AGP track the locus of the poles that start as a complex conjugate pair. The dotted and dotted dashed lines in these plots represent the locus of the pole pair that originates on the real axis. Notice that when a given pole pair is complex, the two poles have the same magnitude but are distinguished in angle. Conversely, when poles lie on the real axis, they have a principal angle of either 180° or 0° corresponding to negative or positive real values, respectively. Furthermore, the GPs show that the system is stable only for a specific range of k, matching that found from the magnitude condition. The ±90° boundaries are marked in the figure in accordance with the criterion presented in equation (9).

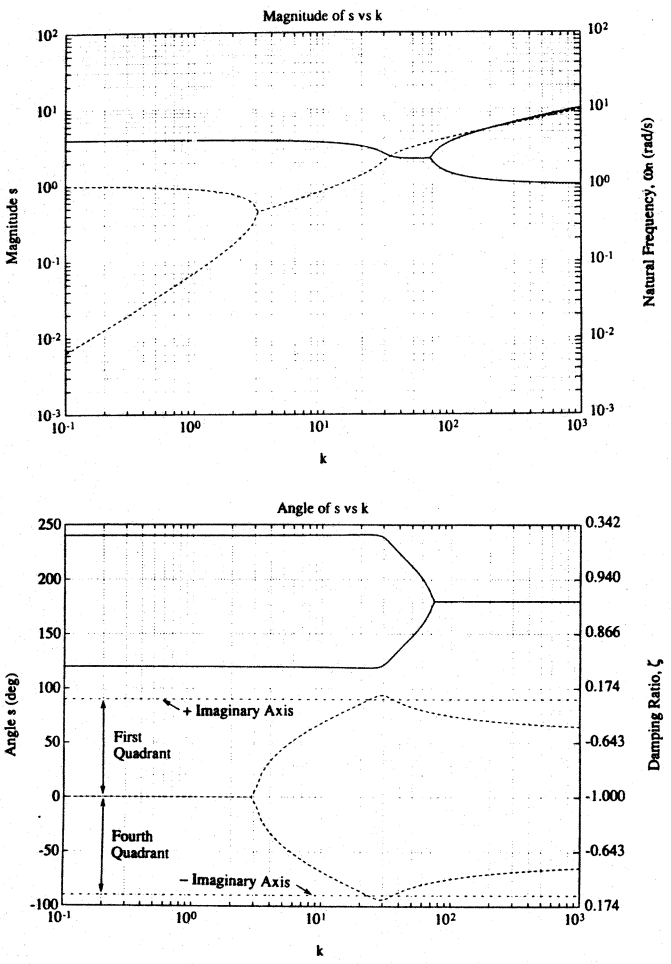

Figure 12. (a) MGP and (b) AGP for Equation (10).

The high gain asymptotes of the root locus are found by examining the AGP for large values of k. The finite zero at s=–1 is identified by the single pole asymptotically approaching unity magnitude at an angle of 180°. The remaining three eigenvalues asymptotically approach infinite zeros at angles ±60° and 180°. For gains higher than those reported in Figure 12, these asymptotes are increasingly prominent.

The slopes of the GPs provide information about the closed–loop system sensitivity to changes in gain. In the example, the system is highly sensitive to gain variations when k is small as evidenced by the rapid change in both the angle and magnitude of the system eigenvalues. This behavior is noticeable at k≈3.1, where the angle of the unstable pole pair rises abruptly. Clearly, as $k \to \infty$ *(i)* the angles in the AGP asymptotically approach the Butterworth configuration, and *(ii)* the magnitudes of the eigenvalues are related to the gain via a power law relationship depicted as a straight line on the MGP (Kurfess and Nagurka, 1991).

MIMO Theory

In the MIMO examples presented below, the system is embedded in the closed–loop feedback configuration of Figure 13. The input–output dynamics are now described by a square transfer function

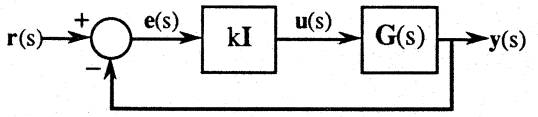

Figure 13. Closed–Loop MIMO Negative Feedback Configuration.

matrix, $\mathbf{G}(s)$, whose elements are transfer functions. For the examples, the controller is $\mathbf{K}(s) = k\mathbf{I}$, implying that each input channel is scaled by the same constant gain k. The internal structure of $\mathbf{G}(s)$ is given by the state–space equations:

$$\dot{\mathbf{x}}(t) = \mathbf{A}\mathbf{x}(t) + \mathbf{B}\mathbf{u}(t) \tag{11}$$

$$\mathbf{y}(t) = \mathbf{C}\mathbf{x}(t) + \mathbf{D}\mathbf{u}(t) \tag{12}$$

where $\mathbf{x}$ is the state vector of length n, $\mathbf{u}$ is the input vector of length m, and $\mathbf{y}$ is the output vector of length, m. Matrices $\mathbf{A}$, $\mathbf{B}$, $\mathbf{C}$ and $\mathbf{D}$ are the system matrix, the control influence matrix, the output matrix, and the feedforward matrix, respectively, with appropriate dimensions. The feedback law

$$\mathbf{u}(t) = k\mathbf{I}\mathbf{e}(t) \tag{13}$$

is specified where the error vector, $\mathbf{e}$, is

$$\mathbf{e}(t) = \mathbf{r}(t) - \mathbf{y}(t) \tag{14}$$

The eigenvalues of the closed–loop system, $s = \lambda_i$ (i=1,2,...,n), are the roots of $\phi_{CL}(s)$, the closed–loop characteristic polynomial,

$$\phi_{CL}(s) = \phi_{OL}(s)\det[\mathbf{I} + k\mathbf{G}(s)] \tag{15}$$

where $\mathbf{G}(s)$ is the transfer function matrix,

$$\mathbf{G}(s) = \mathbf{C}[s\mathbf{I} - \mathbf{A}]^{-1}\mathbf{B} + \mathbf{D} \tag{16}$$

and where $\phi_{OL}(s)$ is the open–loop characteristic polynomial,

$$\phi_{OL}(s) = \det[s\mathbf{I} - \mathbf{A}] \tag{17}$$

By equating the determinant in equation (15) to zero, the MIMO generalization of equation (3) is obtained. The presence of the determinant is the major challenge in generalizing the SISO root locus sketching rules to MIMO systems. The closed–loop system eigenvalues may also be determined from equations (11) – (14) as

$$\lambda_i = \text{eig}[\mathbf{A} - \mathbf{B}(\mathbf{I} + k\mathbf{D})^{-1}k\mathbf{C}] \quad , \quad i = 1, 2, \cdots, n \tag{18}$$

In the examples, the loci of closed–loop eigenvalues are calculated from equation (18) as k is monotonically increased from zero.

Decoupled MIMO Example

The state space representation of this decoupled multivariable system is

$$\dot{\mathbf{x}}(t) = \begin{bmatrix} -1 & 0 \\ 0 & -2 \end{bmatrix}\mathbf{x}(t) + \begin{bmatrix} 1 & 0 \\ 0 & 1 \end{bmatrix}\mathbf{u}(t) \quad , \quad \mathbf{y}(t) = \begin{bmatrix} 1 & 0 \\ 0 & 1 \end{bmatrix}\mathbf{x}(t) \tag{19), (20}$$

corresponding to the transfer function matrix

$$G(s)=\begin{bmatrix}\frac{1}{s+1} & 0\\ 0 & \frac{1}{s+2}\end{bmatrix} \qquad (21)$$

It represents two first order SISO systems with eigenvalues at s={-1, –2}. Since the system is decoupled, the multivariable root locus may be considered to be the superposition of two SISO root locus plots. That is, the MIMO root locus diagram depicts two eigenvalue trajectories, one beginning at s=–1 and the other beginning at s=–2. Both trajectories follow a straight line path along an angle of 180°. Figure 14 presents the root locus for this MIMO decoupled system. Notice that it does not follow the rules of the familiar SISO root locus (*e.g.*, the SISO rule for the portion of the root locus on the real axis is violated), and is not intuitive.

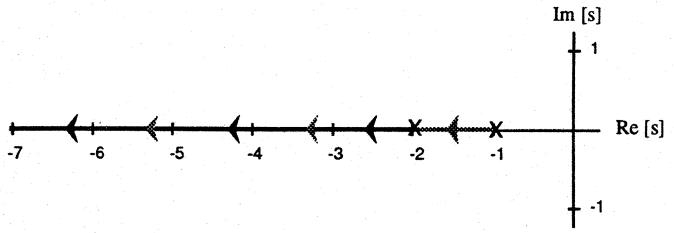

Figure 14. Root Locus for System Given by Equations (19) – (21).

Figure 15 is the MGP for this decoupled MIMO system. Although not shown, the AGP indicates that both eigenvalues have angles of 180° for all gains. Thus, the open–loop eigenvalues are at s={–1, -2}. Furthermore, as k increases, both eigenvalues proceed deeper into the left half plane along the negative real axis at the same constant rate. From the MGP, there is no ambiguity as to the number or location of the poles. Thus, the GPs provide significantly more insight into the behavior of the closed–loop system.

Coupled MIMO Example

The plant dynamics of this example are given by the state space model

$$\dot{x}(t)=\begin{bmatrix}-1 & 0\\ 0 & -2\end{bmatrix}x(t)+\begin{bmatrix}2 & 1\\ 3 & 2\end{bmatrix}u(t)\ ,\ y(t)=\begin{bmatrix}-1 & 1\\ -3 & 2\end{bmatrix}x(t) \qquad (22),\ (23)$$

corresponding to the transfer function matrix

$$G(s)=\begin{bmatrix}\frac{(s-1)}{(s+1)(s+2)} & \frac{s}{(s+1)(s+2)}\\ \frac{-6}{(s+1)(s+2)} & \frac{(s-2)}{(s+1)(s+2)}\end{bmatrix} \qquad (24)$$

(Equation (24) is used as an example by Postlethwaite and MacFarlane, 1979, and later by Yagle, 1981.) This MIMO system has eigenvalues at s={–1, –2}. Since the system is coupled, the multivariable root locus is more complicated than superimposed SISO root locus plots. The MIMO root locus diagram shown in Figure 16 depicts two eigenvalue trajectories, one beginning at s=–1 and the other beginning at s=–2. As in the decoupled example, the eigenvalue at s=–2 follows a negative real axis trajectory. The eigenvalue at s=–1 does not follow the same trajectory. It initially migrates to the right, proceeding to s=1/24 ≈ 0.042, and then reverses. As k is increased, the pole moves back to the left of the imaginary axis. For all values of k, both eigenvalues are purely real. Notice that Figure 16 does not follow the rules of the familiar SISO root locus, and is counter intuitive.

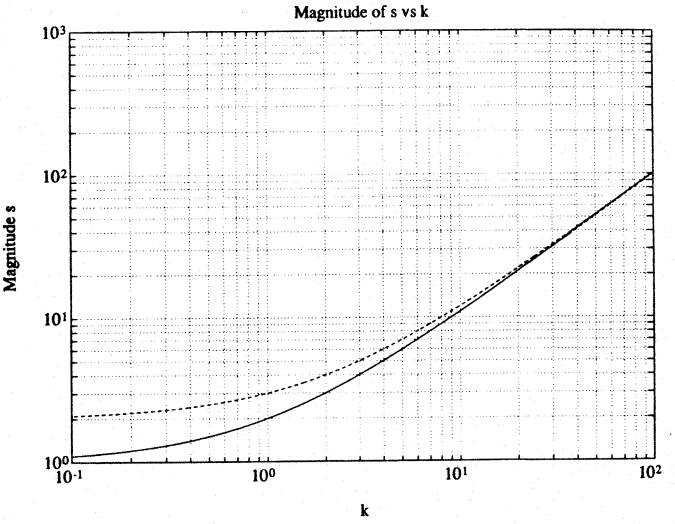

Figure 15. MGP for System Given by Equations (19) – (21).

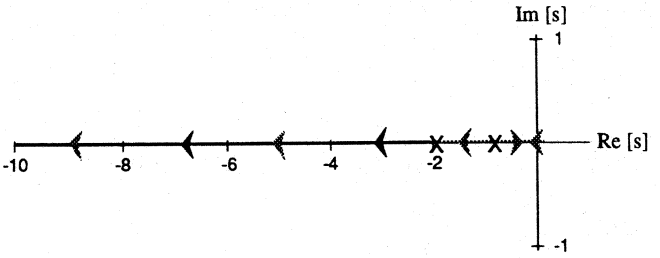

Figure 16. Root Locus for System Given by Equations (22) – (24).

Figure 17 presents the GPs for the coupled MIMO system. It is clear that gain values in the range $1 \le k \le 2$ yield an unstable closed–loop system. This is known since there is a 180° jump in angle as the eigenvalue passes through the origin, highlighting the stable–unstable transition.

The standard root locus plot of this coupled MIMO example is confusing because of the collapse of the Riemann surface into a single complex plane. Since the plot is drawn in two dimensions, branch points may be generated by more than one gain value and, therefore, may not be uniquely presented. The GPs, however, display eigenvalue magnitude and angle information in an unambiguous and concise manner.

Conclusions

The Gain Plots are a set of illuminating plots that expand and enhance the control engineers' design tool set. Just as the Bode plots add a "frequency dimension" to the Nyquist diagram. The GPs are designed to augment the root locus by exposing the "gain dimension." As such, the GPs are the gain domain analogy to the frequency domain Bode plots.

Figure 18 highlights the correspondence of four classical controls graphical tools. As shown, the GPs fill what may be viewed as a

"missing" quadrant of the classical controls tool set. The first row portrays the Nyquist diagram and the Evans root locus spanning a two–dimensional complex plane. The second row shows the Bode plots and GPs spanning a three–dimensional (real) space. The columns show the variable that is used to increase the dimension, *i.e.*, frequency for Bode plots, gain for GPs.

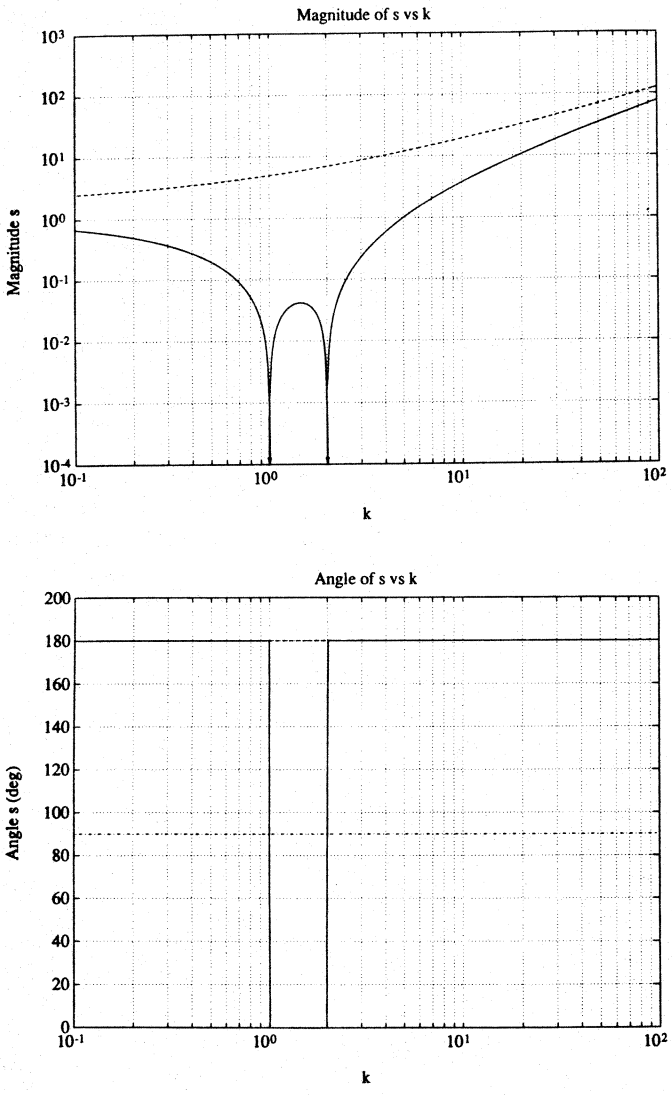

Figure 17. (a) MGP and (b) AGP for Equations (22) – (24).

The GPs enhance the root locus by explicitly portraying the relationship between the gain and the location of each eigenvalue whose trajectories are mapped by the root locus. This information is not readily available from the root locus. The enhancement enables the control designer to identify, by observation, an eigenvalue location with a specific gain, and hence directly view the influence of the gain on stability as well as on system performance. Furthermore, the slopes of the GPs provide a direct measure of eigenvalue gain sensitivity.

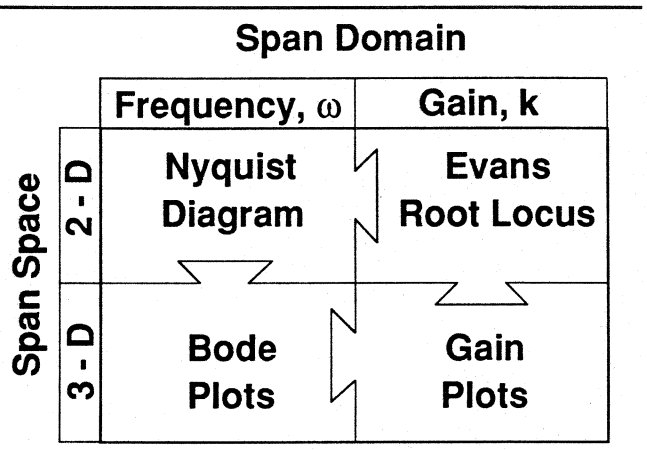

Figure 18. Quadrant Representation of Graphical Control Tools.

Many similarities and differences exist between the root locus and the GPs. For example, both the root locus plot and the GPs can be drawn for systems with transportation lags or dead time. Unlike the root locus plot, the GPs explicitly highlight open–loop poles near or at transmission zeros. These poles are depicted as horizontal lines indicating constant magnitude and angle for all gains. In the root locus plot pole–zero cancellations are normally camouflaged.

Finally, the GPs offer significant advantages over standard root locus plots for MIMO systems. Whereas MIMO root locus plots do not necessarily show unique trajectories, as some branches may overlap, the GPs are a unique description of the eigenvalues. They provide a broad spectrum of information about closed–loop control systems, including stability, performance, and robustness attributes, and are a recommended addition to the control engineers' tool set.

Acknowledgement

The authors are grateful to Professors H.M. Paynter and U. Tasch for their valuable suggestions and encouragement.

References

Bode, H. W., 1940, "Relations Between Attenuation and Phase in Feedback Amplifier Design," Bell System Technical Journal, Vol. 19, pp 421–454.

Evans, W. R., 1948, "Graphical Analysis of Control Systems," Transactions of the American Institute of Electrical Engineers, Vol. 67, pp 547–551.

Evans, W. R., 1950, "Control System Synthesis by Root Locus Method," Transactions of the American Institute of Electrical Engineers, Vol. 69, pp 1–4.

Kurfess, T. R. and Nagurka, M. L, 1991, "Understanding the Root Locus Using Gain Plots," IEEE Control Systems Magazine, August.

Nyquist, H., 1932, "Regeneration Theory," Bell System Technical Journal, Vol. 11, pp 126–147.

Ogata, K., 1990, Modern Control Engineering, Prentice Hall, Englewood Cliffs, NJ.

Postlethwaite, I. and MacFarlane A. G. J., 1979, A Complex Variable Approach to the Analysis of Linear Multivariable Feedback Systems, Lecture Notes in Control and Information Science, Springer–Verlag, New York, NY.

Yagle, A.E., 1981, Properties of Multivariable Root Loci, S.M. Thesis, Department of Electrical Engineering and Computer Science, Massachusetts Institute of Technology, Cambridge, MA.